

Dosimetric Impact of Respiratory Motion During Breast Intensity-modulated Radiation Therapy Using Four-dimensional Dose Calculations

YOUNG EUN CHOI¹, KIHOO SUNG¹, KAP SANG DONG¹, HYUN JU KIM¹ and YOUNG-KHI LIM²

¹Department of Radiation Oncology, Gachon University Gil Medical Center,
Gachon University School of Medicine, Incheon, Republic of Korea;

²Department of Radiological Science, Gachon University, Seongnam, Republic of Korea

Abstract. *Background/Aim:* The use of intensity-modulated radiation therapy (IMRT) in the treatment of breast cancer is increasing worldwide. Despite clear benefits concerning normal tissue sparing and dose homogeneity, the effects of breathing motion and setup error during breast IMRT should be considered. This study aimed to assess the dosimetric impact of respiratory motion on breast IMRT using four-dimensional (4D) dose calculations. *Patients and Methods:* Multiple computed tomography datasets acquired in three representative respiratory amplitudes, were retrospectively re-planned. Based on the reference dose distribution (RDD), motion-adjusted dose distributions (MDD) were recalculated. All 4D dose distributions were calculated by the voxel-based accumulation of RDD and MDD using five temporal probabilities. The dosimetric parameters of the 4D plans were compared to those of RDD. *Results:* The dosimetric parameters of the planning target volume (PTV) were not significantly different between the RDD and 4D plans. Of the parameters of tumor bed (TB) simultaneous-integrated boost (SIB), the mean dose and $V_{95\%}$ for the 4D plans were significantly reduced compared to those of RDD, and the percentage difference in the TB $V_{95\%}$ ranged from -1.1% to -5.7% ($p < 0.05$). *Conclusion:* The breast IMRT plan was robust against respiratory motion during tidal breathing. However, special considerations should be made when designing the TB SIB.

This article is freely accessible online.

Correspondence to: KiHoon Sung, MD, Ph.D., Department of Radiation Oncology, Gachon University Gil Medical Center, 21 Namdong-daero 774beon-gil, Namdong-gu, Incheon 21565, Republic of Korea. Tel: +82 324608052, Fax: +82 324602384, e-mail: novalis@gilhospital.com

Key Words: 4D dose calculation, breast cancer, IMRT, respiratory motion, deformable image registration.

Breast cancer is a heterogeneous disease with different molecular subtypes. Advanced genomic technologies have allowed precision medicine through accurate patient stratification, thereby avoiding unnecessary treatment such as cytotoxic chemotherapy in selected cases of hormone-receptor-positive early breast cancer (1-3). Even in the era of genomic profiling, radiotherapy is an essential component of breast cancer treatment.

Postoperative whole-breast irradiation (WBI) has traditionally been delivered using the conventional tangential field (cTF) technique. However, this technique usually involves incidental irradiation of the heart and lungs, which implies an increased risk of late toxicity (4, 5). Therefore, various normal tissue sparing radiotherapy techniques have been introduced, and intensity-modulated radiation therapy (IMRT) is a widely accepted alternative, especially when treating nodal regions. Breast IMRT allows for the radiation dose to conform more precisely to the breast tissue while limiting the irradiation of normal tissue. Moreover, a more homogeneous dose distribution can be achieved compared to the conventional technique (6).

Despite clear benefits concerning normal tissue sparing and dose homogeneity, the effects of breathing motion and setup error during breast IMRT should be considered (7-12). Inter-fractional setup errors can be reduced by using setup verification and correction techniques, for example, the electric portal imaging device (EPID) and cone-beam computed tomography (CBCT) (7). However, such techniques applied to breast IMRT cannot promise to minimize respiration-induced organ movement and target deformation, which may result in significant dose blurring and differences between the planned and delivered dose distributions (9-12). An approach using four-dimensional (4D) dose calculations was introduced to simulate actual delivered dose distribution throughout the course of the treatment. It can be understood as a weighted summation of dose distributions that correspond to each phase or amplitude of the respiratory cycle (13-15).

The radiotherapy process starts with the acquisition of a computed tomography (CT) image set in the treatment position. This provides a three-dimensional model on which a treatment plan can be generated. Due to respiration-induced changes in organ position, size or shape, the treatment plan based on a single snapshot CT model does not guarantee the actual delivered dose distribution during the treatment session. Multiple CT image datasets should be acquired using 4D CT scanning or respiration-hold technique to account for complete changes during a respiration cycle. The acquired datasets are then reconstructed to generate three-dimensional CT (3D CT) datasets for each respiratory phase or amplitude using the phase-sorting or amplitude-sorting method (14, 16, 17).

The first step in the 4D dose calculation is the generation of a treatment plan for a reference 3D CT dataset as a reference dose distribution (RDD). The RDD is usually generated for the end-expiratory CT dataset. Second, the dose distribution for each 3D CT dataset is recalculated using the same planning parameters used in the RDD and is deformed to a motion-adjusted dose distribution (MDD) using deformable image registration (DIR). Finally, the 4D dose distribution can be calculated by summing the MDDs according to the corresponding temporal probabilities. Temporal probability is defined as the fraction of time spent in each respiratory phase or amplitude (13-15).

In our Institution, a deep-inspiration breath-hold (DIBH) technique is currently used as a standard treatment protocol for left-sided breast cancer patients at risk of cardiac exposure, estimated by the cardiac risk index (18, 19). Participants in this protocol underwent three CT scans, acquired at end-expiration (EE), end-inspiration (EI), and deep-inspiration (DI). In this study, each of these CT datasets was used to compute the 3D dose distributions that correspond to each amplitude of the respiratory cycle (EE, EI, and DI). First, we investigated the differences in dosimetric uncertainty between the cTF technique and IMRT using these 3D dose distributions. Next, the 4D dose distributions were calculated by summing the 3D dose distributions using various temporal probabilities. This study aimed to simulate the actual delivered dose distribution throughout the course of radiation treatment using 4D dose calculations and evaluate the dosimetric impact of respiratory motion on breast IMRT.

Patients and Methods

The data analyzed in this study were based on CT datasets for ten consecutive patients with left-sided breast cancer treated according to our Institutional DIBH protocol. These CT datasets were used to generate treatment plans using the cTF and IMRT technique for this study, retrospectively.

Institutional DIBH protocol and CT acquisition. In our previous studies, we reported the application of the DIBH protocol that was designed to minimize the risk of cardiac mortality and facilitate the

selective use of heart-sparing RT technique (18). Briefly, selecting candidates for DIBH treatment involves two main processes: CT acquisition and estimation of the risk of cardiac mortality. Patients who had been referred to adjuvant radiation therapy after breast-conserving surgery for early-stage left-sided breast cancer underwent a free-breathing (FB) CT scan in the treatment position. Immediately after the CT scan, the risk of cardiac mortality was estimated by the CRI, a directly measurable surrogate from the CT images (19). Selected patients for the DIBH protocol were introduced and trained for Real-time Position Management (RPM; Varian, Palo Alto, CA, USA) and in-house self-respiration monitoring (SRM) systems (18). After completing about 15 min of training, each patient underwent three consecutive CT scans with a slice thickness of 3 mm. Using the RPM system, multiple CT scans were performed in distinct amplitudes of the respiratory cycle, including EE, EI, and DI, respectively.

Delineation and DIR of anatomical structures. Anatomical structures were delineated using the Eclipse treatment planning system (version 13.0; Varian, Palo Alto, CA, USA), as described in our previous study (18). For each of the multiple CT scans, normal structures were delineated. For each patient, we delineated breast target volumes (TVs) only on the EE-CT dataset. The TVs delineated on the EE-CT were deformably registered to the EI-CT and DI-CT datasets for consistency across multiple CT scans (Figure 1a and b). The tumor bed (TB) was defined by surgical clips and/or an associated seroma. The planning target volume (PTV) was delineated to encompass the visible breast tissue and the TB, being limited by the outer contour of the ribs and 5 mm from the skin contour. The anatomic landmarks of the midline (medial), anterior border of the serratus anterior (lateral), inferior border of the clavicle (superior), and 1 cm below the inframammary fold (inferior) were also used to define the PTV. DIR was performed using the Mirada RTx (version 1.6, Mirada Medical, Oxford, UK) and corrected manually with surgical clips if needed.

Treatment planning. Treatment planning was performed in the Eclipse system with the Varian Novalis Tx linear accelerator with the planning objectives listed in Table I. For cTF plans, a pair of wedged tangential fields was used with 6 MV photon half-beams with 2 cm of flash on the anterior breast skin. The prescription to PTV was 50 Gy in 25 fractions. The cTF plans were optimized to ensure that the volume coverage was maintained between 95% and 110% of the prescribed dose for TB and between 90% and 110% for PTV. A single-field electron beam was used in the boost to the TB after WBI. The boost plans were optimized to cover the TB with 95%-105% of the prescribed dose.

For IMRT plans, the same beam angles were used as the cTF plans consisting of two opposed tangential beams of 6 MV. After creating the open field plan, up to five additional fields were manually created and an angle of 20-30° was used between the two beams. The dose was prescribed as 50 Gy in 25 fractions to the PTV and 2.3 Gy per fraction with simultaneous integrated boost (SIB) to the TB. IMRT planning was optimized to cover at least 95% of each PTV by 95% of the prescribed PTV dose, and 100% of TB by 80% of TB prescribed dose. For organs-at-risk, less than 5% of the heart may receive >20 Gy, and less than 15% of the ipsilateral lung may receive >20 Gy. The mean dose to the contralateral breast should be limited to less than 5 Gy (Table I). All plans were generated in EE-CT and then were normalized such that 95% of PTV received 95% of the prescribed dose or higher.

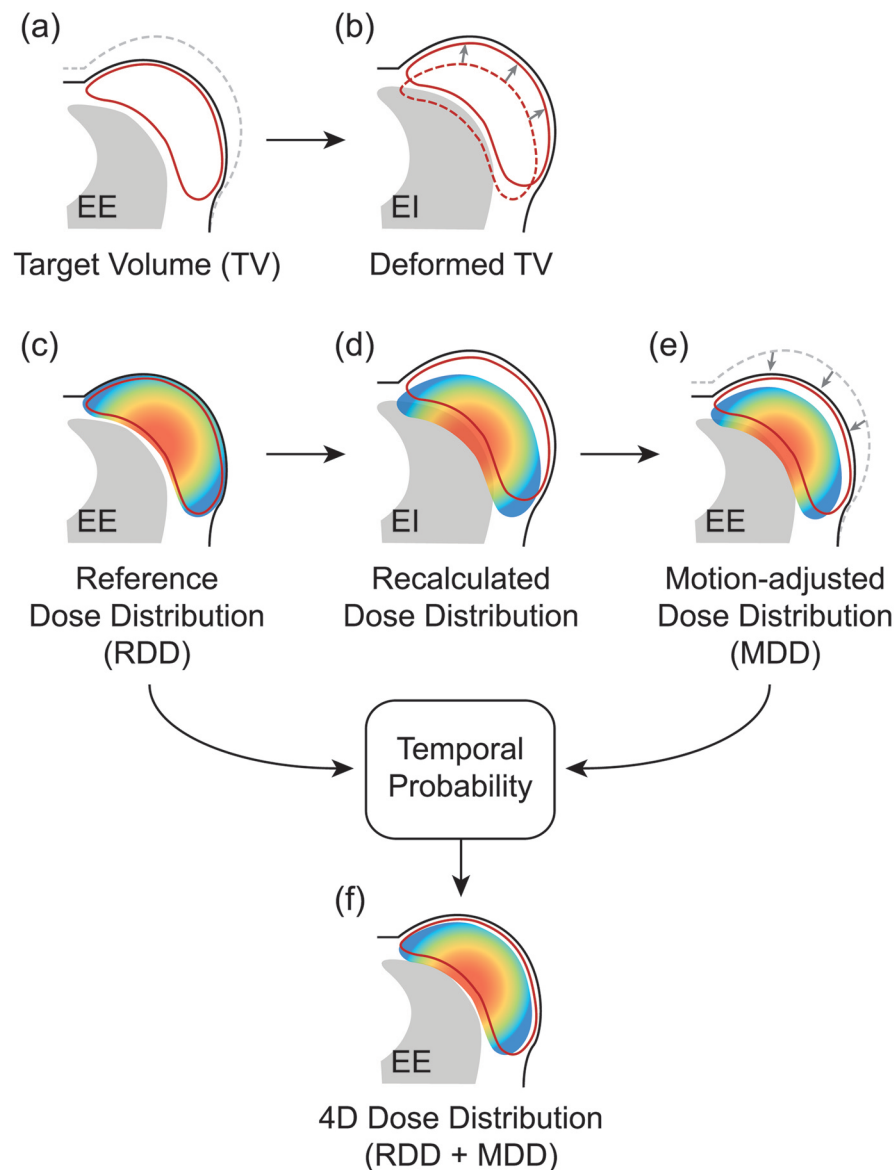


Figure 1. Flowchart outlining the analysis procedures performed in this study. (a) Delineation of the target volume (TV, red lines) on the end-expiration (EE) CT dataset, (b) deformable registration of TV to the end-inspiration (EI) CT datasets, (c) generation of the reference dose distribution (RDD, a transparent color-wash) on EE-CT, (d) recalculation of the dose distribution for the EI-CT dataset using the same planning parameters as those used in the RDD (e) deformable registration of the recalculated dose distribution to EE-CT (motion-adjusted dose distribution; MDD), and (f) 4D dose distribution, weighted summation of the RDD and MDD using temporal probability.

Three-dimensional dose calculation. For each cTF and IMRT plan, a static 3D dose distribution was generated for the EE-CT datasets and was designated as the RDD (Figure 1c). The 3D dose distributions of two inspiratory amplitudes were recalculated using the same planning parameters used in the RDD (Figure 1d). Four-dimensional dose calculation. For IMRT plans, 4D dose distributions were calculated using five temporal probabilities. The CT datasets obtained at EE and EI can estimate the maximum and minimum amplitudes during tidal breathing. The relatively shallow depth of breast motion allowed for the temporal probability to be simplified into only the two-phase

function of EI and EE (11). Since patients spend more time in the expiration phase than in the inspiration phase, the ratio of EE to EI used to generate two-phase temporal probability was defined as 1:1, 2:1, 3:1, 4:1, and 5:1 (Figure 2).

To perform the voxel-based accumulation of the 3D dose distributions, the dose distribution recalculated to EI-CT was deformably registered on EE-CT (Figure 1e), resulting in MDD. Finally, the 4D dose distribution was calculated by summing the 3D dose distributions (RDD and MDD) using respective weighting with respect to five temporal probabilities (Figure 1f).

Table I. Summary of the planning parameters used to generate cTF and IMRT plans using reference CT dataset acquired during the end-expiration (EE) breath-hold maneuver.

	cTF	IMRT
Prescription		
PTV	50 Gy/25 fx.	50 Gy/25 fx.
Tumor bed	10 Gy/5 fx. (Boost after WBI)	57.5 Gy/25 fx. (SIB)
Target coverage		
PTV	90%-110% of Rx	$V_{95\%}=95\%$
Tumor bed	95%-110% of Rx	
Treatment planning		
Field	2 wedged tangential fields (PTV) 1 electron field (tumor bed boost)	6 (3 patients), 7 (7 patients)
Energy	6 MV photon 6, 9, and 12 MeV electron	6 MV photon
Monitor unit (MU/fx.)	536 (473-582)	1,442 (1058-1798)
BOT (sec/fx.)	54 (47-58)	144 (106-180)
Respiration during BOT (breath/fx.)	19 (17-21)	52 (37-63)
Dose constraint		
Heart	$V_{5Gy}<50\%$ $V_{25Gy}<10\%$	mean<5 Gy $V_{20Gy}<5\%$
Ipsilateral lung	$V_{10Gy}<30\%$ $V_{20Gy}<40\%$ $V_{30Gy}<30\%$	mean<15 Gy $V_{20Gy}<15\%$ $V_{30Gy}<5\%$
Contralateral lung		mean<2.5 Gy $V_{5Gy}<5\%$
Contralateral breast	$V_{5Gy}<15\%$	maximum<5 Gy

cTF, Conventional tangential field; IMRT, intensity-modulated radiation therapy; PTV, planning target volume; SIB, simultaneous integrated boost; WBI, whole breast irradiation; fx., fraction; Rx, prescription; V_x , relative organ volume receiving more than a threshold dose (x); BOT, beam on time.

Dosimetric comparison and the impact of respiratory motion. Dosimetric parameters were compared using the plan for EE-CT (RDD) as a reference. Dose-volume histograms (DVHs) were produced for the TB, PTV, heart, lung, and contralateral breast. The relative organ volume receiving more than the threshold dose (x) of each structure (V_x) was calculated. The mean dose of each structure was also calculated.

With regard to targets, we evaluated the conformation number (CN), Radiation Therapy Oncology Group conformity index (CI), lesion coverage factor (CVF), and homogeneity index (HI) (20, 21). $CN=(TV_{ref}/TV) \times (TV_{ref}/V_{ref}) \times 100$, where TV_{ref} represents the TV covered by the reference isodose, TV is the target volume, and V_{ref} is the total volume covered by the reference isodose. $CI=(V_{ref}/TV) \times 100$, and $CVF=(TV_{ref}/TV) \times 100$. The reference isodoses for the TB and PTV were 57.5 Gy and 47.5 Gy, respectively. $HI=D_2/D_{98}$, where D_2 represents the minimum dose received by 2% of the TV, and D_{98} represents the minimum dose received by 98% of the TV.

Statistical analysis. Statistical analysis was performed using R Statistical Software (version 3.3.3; R Foundation for Statistical Computing, Vienna, Austria). A Wilcoxon signed-rank test was used to compare the dosimetric parameters using the EE plan as a reference. A two-tailed p -value<0.05 was considered statistically significant.

Results

Respiratory patterns detected by the RPM system during CT scans are shown in Figure 3a-c. The quality of breath-hold was correct and sufficient to estimate respiratory breast motion during breast radiotherapy in all patients.

Three-dimensional dose distribution. The 3D dose distributions of the cTF and IMRT plans are displayed on CT images as a color-wash overlay in Figure 3. The RDD generated using the EE-CT dataset and the recalculated dose distributions for the EI- and DI-CT datasets were superimposed onto the TVs. The 3D dose distributions of the cTF plans showed no difference among the three different respiratory amplitudes with respect to target coverage and dose distribution (Figure 3d-f). In contrast, the 3D dose distributions of the IMRT plans demonstrated decreased target coverages in the recalculated dose distributions compared with the RDD (Figure 3g-l). The dose distributions representing inspiration periods (EI and DI) showed underdosage in the peripheral region of the PTV near the skin due to the expansion of the body surface (Figure 3h, i, k, and l).

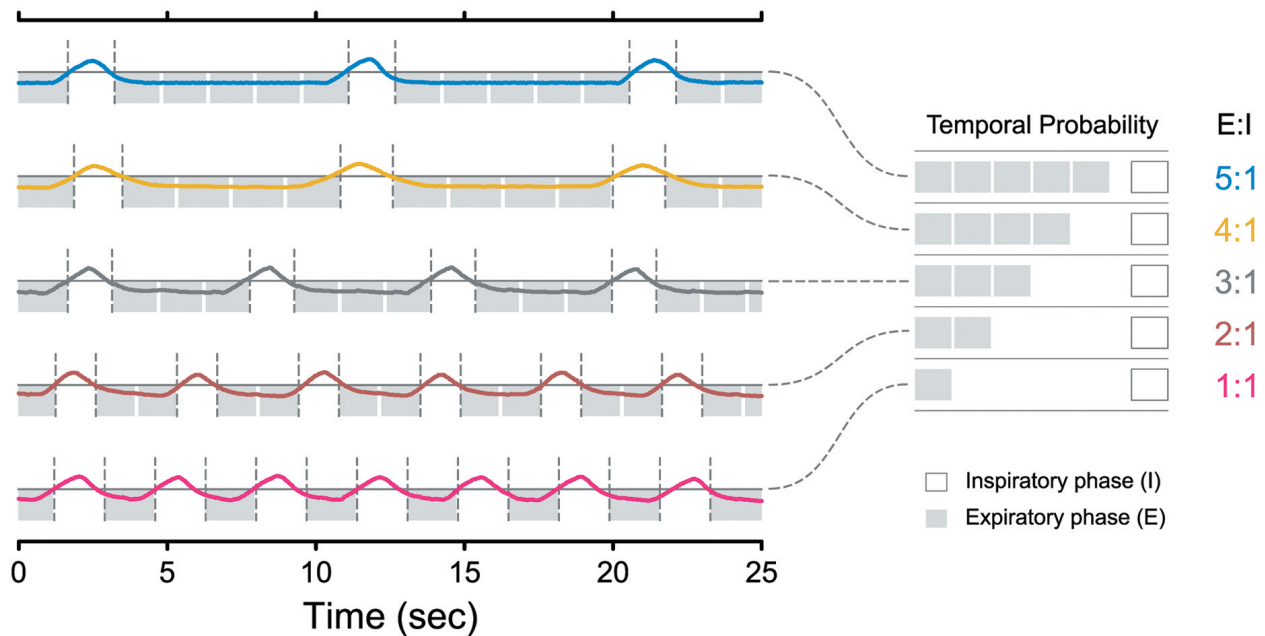


Figure 2. Temporal probability, defined as the fraction of time spent in each respiratory amplitude.

The reddish region receiving the SIB dose (>57.5 Gy) of the IMRT plan was highly conformal to the TB (yellow line) in the RDD (Figure 3g and j), whereas those in the EI and DI amplitudes appeared similar in size and shape but in the wrong locations (Figure 3h, i, k and l).

Table II lists the dosimetric parameters for the 3D dose distributions for each respiratory amplitude and each planning technique, averaged over all patients. For the cTF plan, the dosimetric parameters pertaining to the PTV and TB did not differ significantly among the breathing phases. On the other hand, the doses to the PTV and TB in the IMRT technique were significantly decreased on the inspiration periods, compared to the expiration period. The conformity numbers (CNs) of the PTV for the EE, EI, and EI-plans were 77.8%, 68.7%, and 54.2%, respectively. The CNs of TB yielded relatively larger differences among the three breathing positions, representing an average of 71.7%, 41.1%, and 10.0% for the EE, EI, and EI-plans, respectively. Regardless of the technique, the doses to the ipsilateral lung (mean, $V_{5\text{Gy}}$, $V_{10\text{Gy}}$, and $V_{20\text{Gy}}$) for the EI and DI plans were significantly higher than that of the EE plan.

4D dose distribution. Table III and Figure 4 summarize the average percentage differences between the reference 3D dose distribution (RDD) and 4D dose distributions calculated by five different temporal probabilities in the dosimetric parameter of breast IMRT plans. Of the dosimetric parameters related to the PTV, the mean dose, $V_{90\%}$, CVF,

and HI remained constant throughout the five 4D dose distributions. The CNs for the PTV, on the other hand, demonstrated significantly higher values in 4D dose distributions, and the percentage differences were decreased as the ratio of EE to EI decreased (Figure 4a). Conversely, significant decreases in the CIs for the PTV were observed, and the differences increased with the increasing ratio of the EI component (Figure 4a).

There were significant reductions in the dosimetric parameters for TB, except for $V_{90\%}$ and HI (Table III). The percentage differences in mean TB dose ranged from -0.7% to -1.5%, and those in the three conformity indices ranged from -3.3% to -13.0% (Figure 4b). While significant increases in the dosimetric parameters of the ipsilateral lung were found in the 4D dose distributions, no differences were observed in those of other normal tissues (Figures 4c and 4d).

The dosimetric impact of respiratory motion on breast IMRT is visualized by the DVH of the IMRT plans generated by 4D dose calculation using five different respiratory patterns (Figure 5). The DVHs of a representative patient are shown in Figure 5a, and it can be observed that target coverage ($V_{90\%}$ and $V_{95\%}$) for the TB remarkably decreased as the inspiratory component increased, indicating increased dose inhomogeneity.

The average DVHs for all ten patients are shown in Figure 5b. Compared to the EE plan (solid blue line), the target coverages for the PTV of the 4D plans were diminished, but the differences of $V_{90\%}$ for the PTV were not statistically

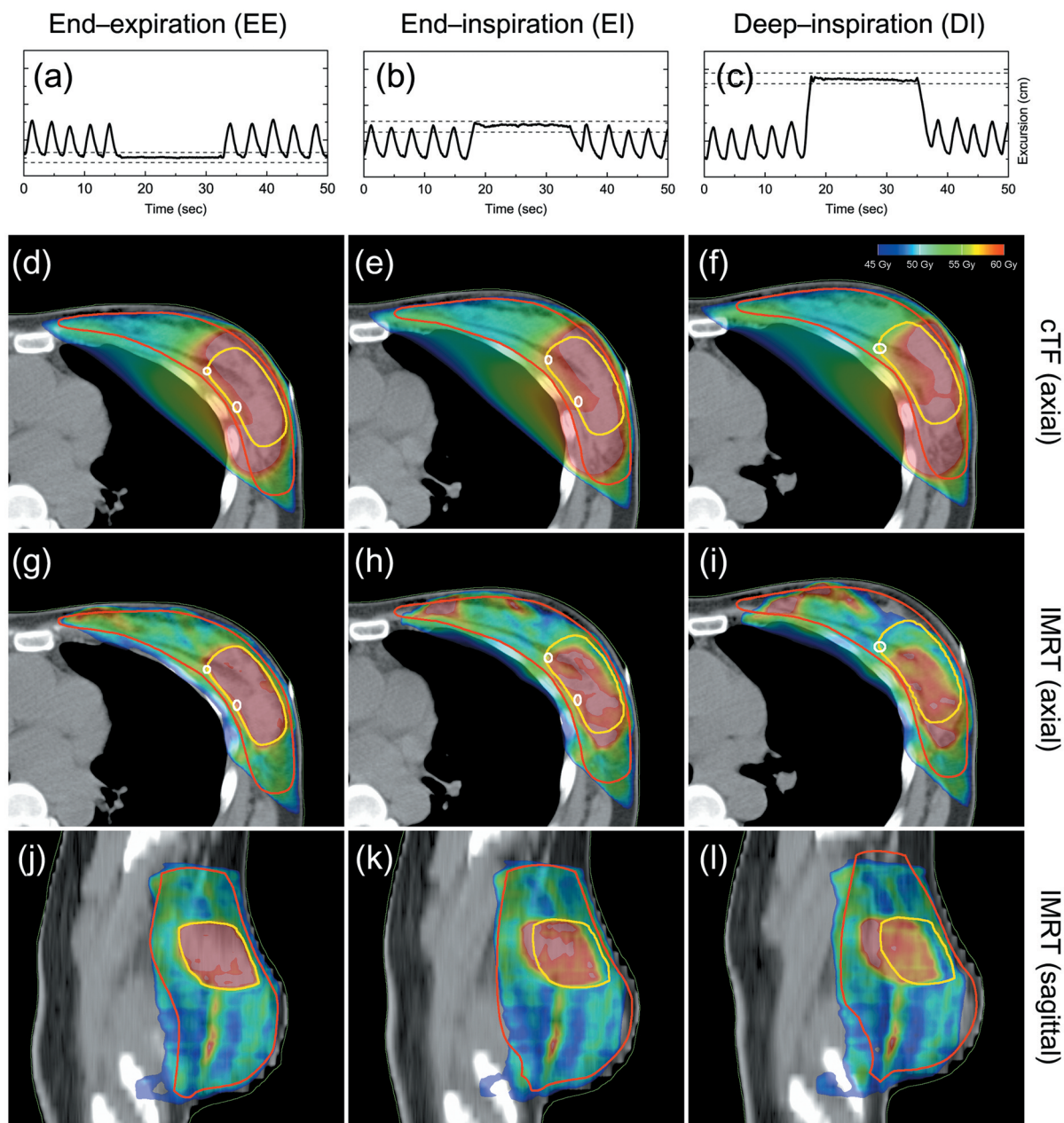


Figure 3. Respiratory patterns for a representative patient detected by the Real-time Position Management (RPM) system during CT scans with different breathing maneuvers including (a) end-expiration (EE), (b) end-inspiration (EI), and (c) deep-inspiration (DI) breath-hold. The 3D dose distributions of the cTF (d-f) and IMRT (g-l) plans were displayed as a color-wash overlay. The red, yellow, and white lines outline the planning target volume (PTV), tumor bed (TB), and clip, respectively. cTF, Conventional tangential field; IMRT, intensity-modulated radiation therapy.

significant (Table III). On the other hand, a significant reduction in target coverage for TB was also shown in the average DVHs. As the inspiration component ratio increased, the percentage difference in the TB $V_{95\%}$ decreased to a maximum difference of -5.7% for the EE:EI=1:1 (Table III). The TB $V_{90\%}$ also decreased in the 4D plans, but the differences were not statistically significant.

Discussion

Various uncertainties exist with respect to setup variation and breathing-induced organ movement in radiotherapy planning and delivery. These uncertainties are usually handled by applying an appropriate target margin to ensure target coverage. However, during breast radiotherapy planning, the

Table II. Dosimetric parameters for the 3D dose distributions of cTF and IMRT plans generated using EE-CT scans, and recalculated dose distributions to EI- and DI-CT (mean±SD).

	cTF			IMRT		
	EE	EI	DI	EE	EI	DI
PTV						
Mean (Gy)	52.6±0.4	52.7±0.4	52.7±0.6	51.3±0.4	51.1±0.5	49.9±0.8*
V _{90%} (%)	99.0±0.6	99.1±0.8	98.6±0.8	99.5±0.3	97.4±2.7*	89.7±3.5*
CN (%)	49.3±7.7	46.4±7.2	43.2±6.7	77.8±5.0	68.7±8.1*	54.2±7.5*
HI	1.36±0.02	1.36±0.03	1.37±0.04	1.28±0.02	1.37±0.15*	1.85±0.39*
Tumor bed						
Mean (Gy)	61.0±0.5	60.8±0.4	60.8±0.7	58.9±0.8	57.3±1.6*	54.7±1.5*
V _{95%} (%)	99.7±0.9	99.4±1.7	98.6±2.5	99.6±0.8	86.9±13.8*	62.9±10.7*
V _{90%} (%)	100.0±0.0	100.0±0.0	100.0±0.0	100.0±0.0	94.4±9.4*	76.9±8.0*
CN (%)	42.4±10.7	39.7±11.2	36.6±11.1	71.7±10.2	41.1±18.0*	10.0±9.0*
HI	1.10±0.09	1.10±0.08	1.11±0.08	1.10±0.02	1.21±0.11*	1.40±0.12*
Heart						
Mean (Gy)	6.4±1.3	6.0±2.1	5.5±1.8	6.6±1.1	6.5±1.7	6.6±1.4
V _{5Gy} (%)	18.9±5.1	17.7±7.1	16.3±6.3*	49.6±14.4	48.4±15.7	49.3±13.3
V _{10Gy} (%)	11.1±2.9	10.2±4.6	9.0±3.8*	13.5±6.7	13.0±7.6	14.6±7.9
V _{20Gy} (%)	9.0±2.7	8.2±4.3	7.1±3.5	3.9±0.8	3.7±2.7	3.8±2.3
V _{30Gy} (%)	8.0±2.5	7.2±4.1	6.2±3.4	1.7±1.1	1.8±1.7	1.8±1.4
Ipsilateral lung						
Mean (Gy)	12.1±2.6	13.5±2.4*	14.4±2.0*	9.7±2.1	11.4±2.2*	12.8±1.9*
V _{5Gy} (%)	39.0±6.5	43.3±6.7*	46.2±6.5*	55.9±13.9	60.1±11.9*	63.1±11.3*
V _{10Gy} (%)	26.4±5.9	29.9±5.1*	32.2±4.5*	30.3±9.8	34.5±8.6*	38.3±8.1*
V _{20Gy} (%)	20.3±6.1	23.0±5.3*	25.0±4.6*	14.0±4.5	18.0±4.5*	21.7±4.3*
Contralateral lung						
Mean (Gy)	0.4±0.1	0.4±0.1*	0.5±0.1*	3.8±1.5	3.7±1.4*	3.5±1.3*
V _{5Gy} (%)	0	0	0	25.8±17.0	24.4±16.2*	22.4±16.0*
Contralateral breast						
Mean (Gy)	0.7±0.1	0.7±0.1*	0.8±0.1*	1.9±0.4	2.0±0.4	2.2±0.4*
V _{5Gy} (%)	0.0±0.0	0.1±0.1	0.2±0.2	4.8±3.2	6.0±3.7	8.4±4.9*

* $p < 0.05$, based on the Wilcoxon signed-rank test using the EE plan as a reference. cTF, Conventional tangential field; IMRT, intensity-modulated radiation therapy; EE, end-expiration; EI, end-inspiration; DI, deep-inspiration; PTV, planning target volume; CN, conformity number; HI, homogeneity index; V_x, relative organ volume receiving more than a threshold dose (x).

use of a uniform margin to the TV can result in the extension of the breast PTV outside the skin, which is not advisable. In the cTF technique, dose coverage of the breast tissue can be achieved using flash or overshoot, which refers to the expansion of the field border with an extra 1-2 cm beyond the skin surface (22). In this study, the cTF plan calculated for the EE-CT dataset with a 2 cm flash beyond the breast tissue was compared with the plans recalculated for the EI- and DI-CT datasets using the same planning parameters as those used in the cTF plan. These simulation data demonstrated that dose coverages of the PTV and TB remained practically constant regardless of the respiratory amplitude (Table II, Figure 3), confirming that skin flashing of treatment fields might be sufficient to compensate for breathing motion.

For breast IMRT planning, it has previously been reported that breast PTV outside the skin results in an iterative process to increase the dose to air, leading to the failure of IMRT

optimization (23). A number of techniques have been suggested to account for such issues, including virtual bolus and robust optimization (24-26). In the virtual bolus technique, a bolus is used for optimization but removed for dose calculation and treatment (24). The discrepancy of geometries used for each process can cause significant variations between the planned and delivered dose distribution. Meanwhile, various robust optimization methods take into account the probability of a setup error occurrence using probability density functions to ensure the stability of the dose distribution according to setup variation and intra-fractional organ movement (25, 26). Despite these advances, these robust optimization techniques require additional work and specific resources.

Several studies have aimed to quantify the dosimetric impact of respiratory motion during WBI (9-12). These studies have examined the static dose distributions correlated to each peak of the breathing cycle, such as EE, EI, and DI. Even in the study utilizing 4D-CT data, only 3D

Table III. Average percentage differences between the RDD and 4D dose distributions calculated by five different temporal probabilities during breast IMRT (mean±SD).

	Reference			% Difference		
	EE	EE:EI (5:1)	EE:EI (4:1)	EE:EI (3:1)	EE:EI (2:1)	EE:EI (1:1)
PTV						
Mean (Gy)	51.3±0.4	-0.2±0.1	-0.2±0.1	-0.2±0.1	-0.2±0.2	-0.2±0.2
V _{90%} (%)	99.5±0.3	0.0±0.1	0.0±0.1	-0.1±0.1	-0.2±0.3	-0.6±0.9
CN (%)	77.8±5.0	1.7±0.6*	1.6±0.6*	1.4±0.6*	0.9±0.7*	-0.4±1.6
CI (%)	117.0±8.5	-2.5±1.0*	-2.4±1.1*	-2.4±1.2*	-2.2±1.4*	-1.7±1.8*
CVF (%)	95.0±0.0	0.0±0.3	0.0±0.4	-0.1±0.5	-0.3±0.8	-0.9±1.6
HI	1.28±0.02	0.0±0.0	0.0±0.0	0.0±0.0	0.0±0.0	0.0±0.0
Tumor bed						
Mean (Gy)	58.9±0.8	-0.4±0.3*	-0.5±0.4*	-0.5±0.5*	-0.6±0.7*	-0.9±1.0*
V _{95%} (%)	99.6±0.8	-1.1±1.1*	-1.4±1.5*	-2.0±2.4*	-3.0±4.1*	-5.7±8.3*
V _{90%} (%)	100.0±0.0	0.0±0.0	0.0±0.1	-0.1±0.2	-0.2±0.7	-1.2±2.8
CN (%)	71.7±10.2	-3.3±5.3	-4.2±6.5	-5.5±8.6*	-8.0±11.4*	-13.0±16.0*
CI (%)	103.3±25.6	-9.0±5.5*	-9.6±6.6*	-10.2±7.6*	-10.6±9.2*	-10.1±12.1*
CVF (%)	85.0±13.0	-5.7±5.1*	-6.6±6.3*	-7.8±8.0*	-9.6±10.5*	-12.9±14.7*
HI	1.10±0.02	0.0±0.0	0.0±0.0	0.0±0.0	0.0±0.0	0.0±0.0
Heart						
Mean (Gy)	6.6±1.1	0.0±0.1	0.0±0.1	0.0±0.1	0.0±0.2	0.0±0.2
V _{5Gy} (%)	49.6±14.4	0.1±0.4	0.1±0.5	0.0±0.6	0.0±0.8	-0.1±1.2
V _{10Gy} (%)	13.5±6.7	0.0±0.3	0.0±0.4	0.0±0.5	0.0±0.6	-0.1±0.8
V _{20Gy} (%)	3.9±0.8	0.1±0.3	0.0±0.3	0.0±0.4	0.0±0.5	0.0±0.7
V _{30Gy} (%)	1.7±1.1	-0.1±0.2	-0.1±0.2	-0.1±0.3	-0.1±0.3	0.0±0.5
Ipsilateral lung						
Mean (Gy)	9.7±2.1	0.2±0.1*	0.2±0.1*	0.2±0.2*	0.3±0.2*	0.4±0.4*
V _{5Gy} (%)	55.9±13.9	0.5±0.5*	0.6±0.6*	0.8±0.8*	1.0±1.0*	1.5±1.5*
V _{10Gy} (%)	30.3±9.8	0.3±0.3*	0.4±0.3*	0.5±0.4*	0.7±0.5*	1.0±0.7*
V _{20Gy} (%)	14.0±4.5	0.5±0.4*	0.5±0.4*	0.7±0.5*	0.8±0.7*	1.2±0.9*
Contralateral lung						
Mean (Gy)	3.8±1.5	0.0±0.0	0.0±0.0	0.0±0.0	0.0±0.1	0.0±0.1
V _{5Gy} (%)	25.8±17.0	0.0±0.3	0.0±0.3	0.0±0.4	-0.1±0.5	-0.2±0.7
Contralateral breast						
Mean (Gy)	1.9±0.4	0.0±0.0	0.0±0.0	0.0±0.0	0.0±0.0	0.0±0.1
V _{5Gy} (%)	4.8±3.2	-0.2±0.3	-0.2±0.4	-0.2±0.4	-0.1±0.5	0.0±0.6

*p<0.05, based on the Wilcoxon signed-rank test using the EE plan as a reference. RDD, Reference dose distribution; IMRT, intensity-modulated radiation therapy; EE, end-expiration; EI, end-inspiration; PTV, planning target volume; CN, conformity number; CI, Radiation Therapy Oncology Group (RTOG) conformity index; CVF, lesion coverage factor; HI, homogeneity index; V_x, relative organ volume receiving more than a threshold dose (x).

calculation results were evaluated using dosimetric parameters for each respiratory phase (12). Because the shape and position of the TV change continuously during breathing, the actual dose distribution delivered to the patient should be evaluated using a 4D dose calculation (13, 14). In this study, the two-phase temporal probabilities of EE and EI were used to simulate various breathing patterns. According to these temporal probabilities, the static dose 3D distributions were convoluted to generate 4D dose distributions using DIR (Figure 1). Our dosimetric analysis showed that breast PTV was less sensitive to respiratory motion during breast IMRT (Table III, Figure 5). In contrast, the respiratory motion-induced dose blurring on target coverage was dominant for TB SIB (Figure 5). As shown in

Figure 5a, the DVHs for the PTV did not differ significantly among breathing patterns, even in the worst-case scenario for TB coverage. When extrapolating the results of this study, breast IMRT technique produced dose distributions that were robust against breast motion during tidal breathing and could be used without respiration control. However, special considerations should be given to the implication of breast IMRT, particularly when designing the SIB technique for TB. To our knowledge, this is the first study to confirm the motion-induced dose blurring effect on the TB boost in the use of breast IMRT.

A CI is a measure of how well the volume of dose distribution conforms to the size and shape of the TV, where the TV is constant value for each target. Because the

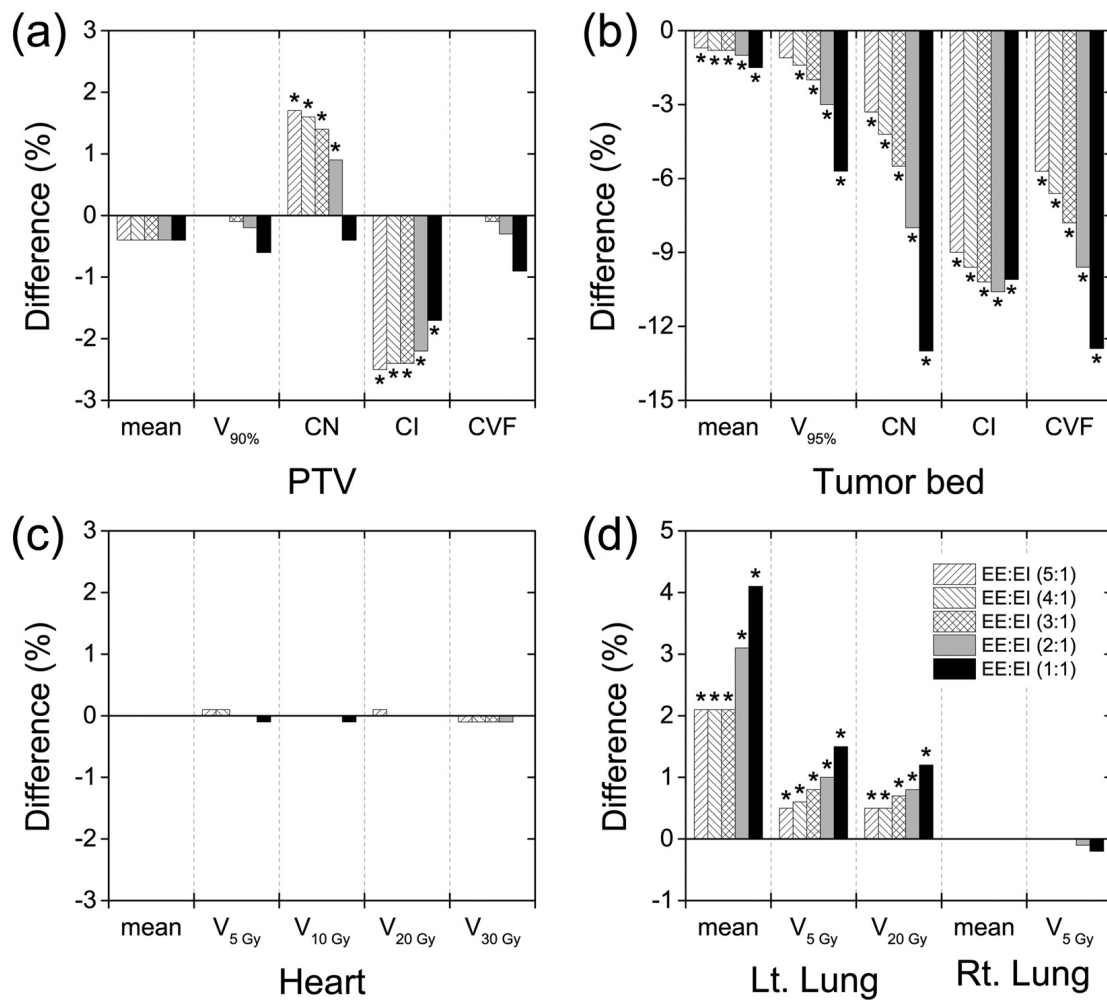


Figure 4. Average percentage differences in the dosimetric parameters of the 4D dose distributions compared with to those of the reference dose distribution for the EE amplitude during breast IMRT. * $p < 0.05$, based on the Wilcoxon signed-rank test using the EE plan as a reference. IMRT, Intensity-modulated radiation therapy; EE, end-expiration; EI, end-inspiration; PTV, planning target volume; V_x , relative organ volume receiving more than a threshold dose (x); CN, conformity number; CI, Radiation Therapy Oncology Group (RTOG) conformity index; CVF, lesion coverage factor.

reference isodose volume (V_{ref}) is relatively constant for each plan evaluated, the TV covered by the reference isodose (TV_{ref}) is the main determinant of dose conformity in comparing rival plans. However, in dosimetric studies using 4D dose calculations, V_{ref} also changes dramatically due to the dose blurring effect caused by target motion. Therefore, conformity indices based on V_{ref} should be carefully interpreted. As shown in Figure 4a, three conformity indices for the PTV revealed paradoxical results among each index and respiratory pattern. This is because the decrease in V_{ref} is larger than that of TV_{ref} according to the respiratory pattern change. Another reason is that V_{ref} is the denominator for CN, but the numerator for CI. Consequentially, the use of the CVF irrelevant to V_{ref} is recommended to investigate the target coverage for the 4D dosimetric study.

This study has several limitations. The calculation of the 4D dose distribution requires the respiratory pattern and CT images of each respiration phase. Ideally, these parameters should be acquired using 4D-CT. In this study, only two respiratory amplitudes corresponding to each peak of the tidal volume (EE and EI) were used to generate temporal probabilities representing various breathing patterns. Considering the shallow depth of breathing amplitude and a short distance of breast movement, the convolution using two-phase temporal probability would be a reasonable representation of reality. However, facilitating 4D-CT would be desirable to derive a more realistic 4D dose distribution. In addition, the effect of respiratory motion for various targets including nodal regions with different IMRT techniques should be investigated.

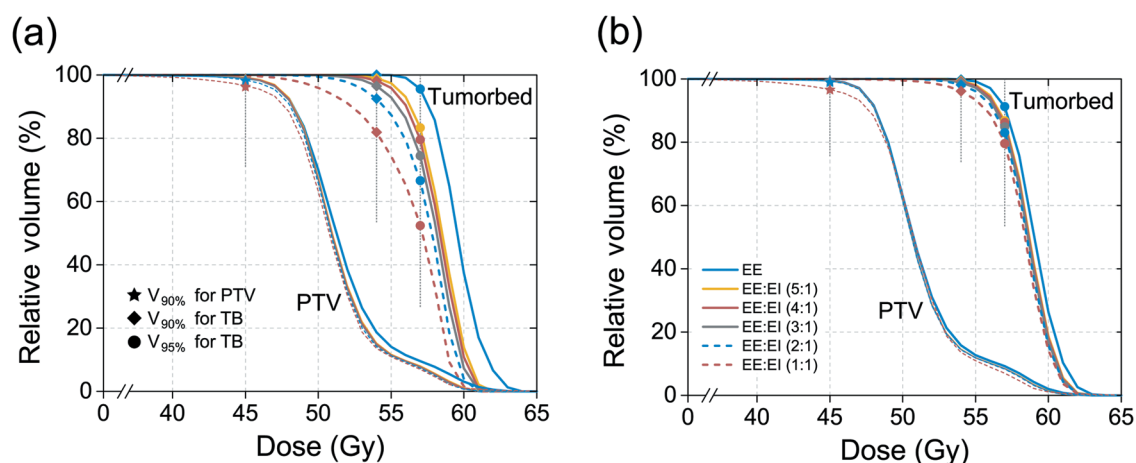


Figure 5. Results of the 4D dose calculations demonstrating respiratory motion-induced dose blurring on target coverage during breast IMRT. Dose-volume histograms (DVHs) for the tumor bed and planning target volume (PTV) were compared using the EE plan as a reference (solid blue lines). (a) DVHs of a representative case and (b) average DVHs for ten patients. IMRT, Intensity modulated radiation therapy; EE, end-expiration; EI, end-inspiration.

Conclusion

This study showed that the actual dose distribution of breast IMRT delivered to the patient, which is closer to the ground truth, could be simulated by 4D dose calculations with DIR. While significant reductions of the target coverage were observed in the TB, only minor differences in the PTV were observed throughout the five respiratory patterns. Special considerations such as breathing-adapted techniques and robust optimization, should be given to the implication of breast IMRT with the TB SIB technique.

Conflicts of Interest

The Authors have no conflicts of interest to declare.

Authors' Contributions

Conceptualization, KS and YEC; methodology and investigation, YEC and KSD; data analysis, KS, YEC and HJK; article writing, YEC and KS; article review, HJK and KSD; article approval, KS and HJK.

Acknowledgements

This work was supported by the Gachon University Gil Medical Center (Grant number: 2017-15).

References

- van't Veer LJ, Dai H, van de Vijver MJ, He YD, Hart AA, Mao M, Peterse HL, van der Kooy K, Marton MJ, Witteveen AT, Schreiber GJ, Kerkhoven RM, Roberts C, Linsley PS, Bernards

- R and Friend SH: Gene expression profiling predicts clinical outcome of breast cancer. *Nature* 415(6871): 530-536, 2002. PMID: 11823860. DOI: 10.1038/415530a
- Curtis C: Genomic profiling of breast cancers. *Curr Opin Obstet Gynecol* 27(1): 34-39, 2015. PMID: 25502431. DOI: 10.1097/gco.0000000000000145
- Varga Z, Sinn P, Fritzsche F, von Hochstetter A, Noske A, Schraml P, Tausch C, Trojan A and Moch H: Comparison of EndoPredict and Oncotype DX test results in hormone receptor positive invasive breast cancer. *PLoS One* 8(3): e58483, 2013. PMID: 23505515. DOI: 10.1371/journal.pone.0058483
- Darby SC, Ewertz M, McGale P, Bennet AM, Blom-Goldman U, Bronnum D, Correa C, Cutter D, Gagliardi G, Gigante B, Jensen MB, Nisbet A, Peto R, Rahimi K, Taylor C and Hall P: Risk of ischemic heart disease in women after radiotherapy for breast cancer. *N Engl J Med* 368(11): 987-998, 2013. PMID: 23484825. DOI: 10.1056/NEJMoal209825
- Hurkmans CW, Borger JH, Bos LJ, van der Horst A, Pieters BR, Lebesque JV and Mijnheer BJ: Cardiac and lung complication probabilities after breast cancer irradiation. *Radiother Oncol* 55(2): 145-151, 2000. PMID: 10799726. DOI: 10.1016/s0167-8140(00)00152-3
- Schubert LK, Gondi V, Sengbusch E, Westerly DC, Soisson ET, Paliwal BR, Mackie TR, Mehta MP, Patel RR, Tome WA and Cannon GM: Dosimetric comparison of left-sided whole breast irradiation with 3DCRT, forward-planned IMRT, inverse-planned IMRT, helical tomotherapy, and topotherapy. *Radiother Oncol* 100(2): 241-246, 2011. PMID: 21316783. DOI: 10.1016/j.radonc.2011.01.004
- Topolnjak R, Sonke JJ, Nijkamp J, Rasch C, Minkema D, Remeijer P and van Vliet-Vroegindeweij C: Breast patient setup error assessment: Comparison of electronic portal image devices and cone-beam computed tomography matching results. *Int J Radiat Oncol Biol Phys* 78(4): 1235-1243, 2010. PMID: 20472368. DOI: 10.1016/j.ijrobp.2009.12.021

- 8 van Mourik A, van Kranen S, den Hollander S, Sonke JJ, van Herk M and van Vliet-Vroegindewij C: Effects of setup errors and shape changes on breast radiotherapy. *Int J Radiat Oncol Biol Phys* 79(5): 1557-1564, 2011. PMID: 20933341. DOI: 10.1016/j.ijrobp.2010.07.032
- 9 Cao J, Roeske JC, Chmura SJ, Salama JK, Shoushtari AN, Boyer AL and Martel MK: Calculation and prediction of the effect of respiratory motion on whole breast radiation therapy dose distributions. *Med Dosim* 34(2): 126-132, 2009. PMID: 19410141. DOI: 10.1016/j.meddos.2008.07.002
- 10 Furuya T, Sugimoto S, Kurokawa C, Ozawa S, Karasawa K and Sasai K: The dosimetric impact of respiratory breast movement and daily setup error on tangential whole breast irradiation using conventional wedge, field-in-field and irregular surface compensator techniques. *J Radiat Res* 54(1): 157-165, 2013. PMID: 22859565. DOI: 10.1093/jrr/rrs064
- 11 George R, Keall PJ, Kini VR, Vedam SS, Siebers JV, Wu Q, Lauterbach MH, Arthur DW and Mohan R: Quantifying the effect of intrafraction motion during breast IMRT planning and dose delivery. *Med Phys* 30(4): 552-562, 2003. PMID: 12722807. DOI: 10.1118/1.1543151
- 12 Wang W, Li JB, Hu HG, Li FX, Xu M, Sun T and Lu J: Correlation between target motion and the dosimetric variance of breast and organ at risk during whole breast radiotherapy using 4DCT. *Radiat Oncol* 8: 111, 2013. PMID: 23638837. DOI: 10.1186/1748-717x-8-111
- 13 Guckenberger M, Wilbert J, Krieger T, Richter A, Baier K, Meyer J and Flentje M: Four-dimensional treatment planning for stereotactic body radiotherapy. *Int J Radiat Oncol Biol Phys* 69(1): 276-285, 2007. PMID: 17707282. DOI: 10.1016/j.ijrobp.2007.04.074
- 14 Rouabhi O, Ma M, Bayouth J and Xia J: Impact of temporal probability in 4D dose calculation for lung tumors. *J Appl Clin Med Phys* 16(6): 110-118, 2015. PMID: 28297522. DOI: 10.1120/jacmp.v16i6.5517
- 15 Kuo HC, Mah D, Chuang KS, Wu A, Hong L, Yaparpalvi R, Spierer M and Kalnicki S: A method incorporating 4DCT data for evaluating the dosimetric effects of respiratory motion in single-arc IMAT. *Phys Med Biol* 55(12): 3479-3497, 2010. PMID: 20508324. DOI: 10.1088/0031-9155/55/12/014
- 16 Lu W, Parikh PJ, Hubenschmidt JP, Bradley JD and Low DA: A comparison between amplitude sorting and phase-angle sorting using external respiratory measurement for 4D CT. *Med Phys* 33(8): 2964-2974, 2006. PMID: 16964875. DOI: 10.1118/1.2219772
- 17 Wink N, Panknin C and Solberg TD: Phase *versus* amplitude sorting of 4D-CT data. *J Appl Clin Med Phys* 7(1): 77-85, 2006. PMID: 16518319. DOI: 10.1120/jacmp.v7i1.2198
- 18 Sung K, Lee KC, Lee SH, Ahn SH, Lee SH and Choi J: Cardiac dose reduction with breathing adapted radiotherapy using self respiration monitoring system for left-sided breast cancer. *Radiat Oncol J* 32(2): 84-94, 2014. PMID: 25061577. DOI: 10.3857/roj.2014.32.2.84
- 19 Sung K, Choi YE and Lee KC: Cardiac risk index as a simple geometric indicator to select patients for the heart-sparing radiotherapy of left-sided breast cancer. *J Med Imaging Radiat Oncol* 61(3): 410-417, 2017. PMID: 28004515. DOI: 10.1111/1754-9485.12567
- 20 Feuvret L, Noel G, Mazeron JJ and Bey P: Conformity index: A review. *Int J Radiat Oncol Biol Phys* 64(2): 333-342, 2006. PMID: 16414369. DOI: 10.1016/j.ijrobp.2005.09.028
- 21 van't Riet A, Mak AC, Moerland MA, Elders LH and van der Zee W: A conformation number to quantify the degree of conformality in brachytherapy and external beam irradiation: Application to the prostate. *Int J Radiat Oncol Biol Phys* 37(3): 731-736, 1997. PMID: 9112473. DOI: 10.1016/s0360-3016(96)00601-3
- 22 McGee KP, Fein DA, Hanlon AL, Schultheiss TE and Fowble BL: The value of setup portal films as an estimate of a patient's position throughout fractionated tangential breast irradiation: An on-line study. *Int J Radiat Oncol Biol Phys* 37(1): 223-228, 1997. PMID: 9054899. DOI: 10.1016/s0360-3016(96)00463-4
- 23 Thomas SJ and Hoole AC: The effect of optimization on surface dose in intensity modulated radiotherapy (IMRT). *Phys Med Biol* 49(21): 4919-4928, 2004. PMID: 15584527. DOI: 10.1088/0031-9155/49/21/005
- 24 Thilmann C, Grosser KH, Rhein B, Zabel A, Wannemacher M and Debus J: Virtual bolus for inversion radiotherapy planning in intensity-modulated radiotherapy of breast carcinoma within the scope of adjuvant therapy. *Strahlenther Onkol* 178(3): 139-146, 2002. PMID: 11962190. DOI: 10.1007/s00066-002-0915-x
- 25 Chan TC, Bortfeld T and Tsitsiklis JN: A robust approach to IMRT optimization. *Phys Med Biol* 51(10): 2567-2583, 2006. PMID: 16675870. DOI: 10.1088/0031-9155/51/10/014
- 26 Byrne M, Hu Y and Archibald-Heeren B: Evaluation of raystition robust optimisation for superficial target coverage with setup variation in breast IMRT. *Australas Phys Eng Sci Med* 39(3): 705-716, 2016. PMID: 27581727. DOI: 10.1007/s13246-016-0466-6

Received October 20, 2020

Revised November 18, 2020

Accepted November 25, 2020